VILNIUS UNIVERSITY

CENTER FOR PHYSICAL SCIENCES AND TECHNOLOGY

Evaldas Stankevičius

FABRICATION OF PERIODIC MICRO-STRUCTURES IN POLYMERS BY INTERFERENCE LITHOGRAPHY AND MODIFICATION OF THEIR PROPERTIES BY PHOTO-GRAFTING TECHNIQUE

Summary of doctoral thesis,
Physical Sciences, Physics (02P)

Vilnius, 2014

Dissertation was prepared in 2009-2013 at the Center for Physical Sciences and Technology (CPST). Part of the experiments was done in Vienna University of Technology (Austria).

Scientific supervisor:

Dr. Gediminas Račiukaitis (*Center for Physical Sciences and Technology* (Lithuania), Physical Sciences - 02P).

Scientific advisor:

Dr. Aleksandr Ovsianikov (*Vienna University of Technology* (Austria), Physical Sciences - 02P).

Doctoral thesis will be defended at the Center for Physical Sciences and Technology in the senate of Physical Sciences:

Chairman:

Prof. habil. dr. Valdas Sirutkaitis (*Vilnius University*, Physical Sciences, Physics - 02P).

Members:

1. Prof. habil. dr. Arūnas Krotkus (*Center for Physical Sciences and Technology*, Physical Sciences, Physics - 02P);

2. Prof. habil. dr. Eugenijus Šatkovskis (*Vilnius Gediminas Technical University*, Physical Sciences, Physics - 02P);

3. Doc. dr. Andrius Melninkaitis (*Vilnius University*, Technology Sciences, Material Engineering - 08T);

4. Dr. Mindaugas Andrulevičius (*Kaunas Technological University*, Physical Sciences, Physics - 02P).

Official opponents:

1. Prof. habil. dr. Alfonsas Grigonis (*Kaunas Technological University*, Physical Sciences, Physics - 02P);

2. Dr. Domas Paipulas (*Vilnius University*, Physical Sciences, Physics - 02P).

This thesis will be under open consideration on 22nd of May, 2014 10 a.m. at the hall of CPST Institute of Physics.

Address: Savanoriu ave. 231, LT-02300 Vilnius, Lithuania.

Summary of doctoral thesis was distributed on 20th of March, 2014.

Doctoral thesis is available at libraries of CPST and Vilnius University.

VILNIAUS UNIVERSITETAS

FIZINIŲ IR TECHNOLOGIJOS MOKSLŲ CENTRAS

Evaldas Stankevičius

PERIODINIŲ MIKRODARINIŲ FORMAVIMAS POLIMERUOSE IR JŲ SAVYBIŲ MODIFIKAVIMAS INTERFERENCINĖS LITOGRAFIJOS IR FOTOĮSKIEPIJIMO METODAIS

Daktaro disertacija,

Fiziniai mokslai, Fizika (02P)

Vilnius, 2014

Disertacija rengta 2009-2013 metais Fizinių ir technologijos mokslų centro lazerinių technologijų skyriuje. Dalis eksperimentų buvo atlikta Vienos technologijos universitete (TU Wien, Viena, Austrija).

Mokslinis vadovas:

Dr. Gediminas Račiukaitis (*Fizinių ir technologijos mokslų centras*, fiziniai mokslai, fizika - 02P).

Konsultantas:

Dr. Aleksandr Ovsianikov (*Vienos technologijos universitetas*, fiziniai mokslai, fizika - 02P).

Disertacija ginama Vilniaus universiteto Fizikos mokslų krypties taryboje:

Pirmininkas:

Prof. habil. dr. Valdas Sirutkaitis (*Vilniaus universitetas*, fiziniai mokslai, fizika - 02P).

Nariai:

1. Prof. habil. dr. Arūnas Krotkus (*Fizinių ir technologijos mokslų centras*, fiziniai mokslai, fizika - 02P);

2. Prof. habil. dr. Eugenijus Šatkovskis (*Vilniaus Gedimino technikos universitetas*, fiziniai mokslai, fizika - 02P);

3. Doc. dr. Andrius Melninkaitis (*Vilniaus universitetas*, technologijos mokslai, medžiagų inžinerija - 08T);

4. Dr. Mindaugas Andrulevičius (*Kauno technologijos universitetas*, fiziniai mokslai, fizika - 02P).

Oponentai:

1. Prof. habil. dr. Alfonsas Grigonis (*Kauno technologijos universitetas*, fiziniai mokslai, fizika - 02P);

2. Dr. Domas Paipulas (*Vilniaus universitetas*, fiziniai mokslai, fizika - 02P).

Disertacija bus ginama viešame Fizikos mokslo krypties tarybos posėdyje 2014 m. gegužės mėn. 22 d. 10 val. FTMC Fizikos instituto salėje.

Adresas: Savanorių pr. 231, LT-02300 Vilnius, Lietuva.

Disertacijos santrauka išsiuntinėta 2014 m. kovo 20 d.

Disertaciją galima peržiūrėti Vilniaus universiteto bibliotekoje.

Contents

Introduction

Here we present results of our experimental work to create periodic micro-structures in polymers by using interference lithography (IL) [1] and their photo-modification by photo-grafting [2]. Interference lithography is a powerful technique which allows fabrication of periodic micro-structures over a large area by a single laser exposure. This technique is based on the recording of the interference pattern into a photosensitive material. Interference lithography technique enables fabricating 2D and 3D periodic structures which can be used as functional devices in many fields: photonics (photonics crystals [3]), tissue engineering (scaffolds for cell growth [4]), micro-fluidics [5], micro-optics (micro-lens arrays [6]), sensors [7], etc.

Other technique demonstrated in this work is photo-grafting. Photo-grafting is a method utilizing light activation for covalent incorporation of functional molecules to a polymer surface or polymer matrix. It has been widely applied as a simple and versatile method for tailoring physical-chemical properties of various surfaces.

Relevance

At present, thanks to modern high technologies, the interest in periodic micro-structures has significantly increased, due to their potential applications in various fields (telecommunications [8], photonics, tissue engineering, micro-optics, etc.). By the formation of periodic micro-structures suitable for a variety of practical applications, it is desirable that exterior dimensions of the fabricated structures should be at least on a millimeter scale and their internal architecture (micrometers or nanometers scale) can be easily controlled. Some technologies (direct laser writing based on photo-polymerization (DLW) [4], 3D printing [9]) allows the fabrication of desired micro-structures with high internal architecture control but only in a limited area and at low fabrication speed. Other technologies (such as solvent casting and particulate leaching [10], phase separation [11] or gas foaming [12] methods) enable quite fast formation of micro-structures in a large area quite quickly but with poor internal geometry control. Meanwhile, the interference lithography is distinguished by both: fast fabrication of micro-structures in a large area and

high internal architecture control. Interference lithography technique is promising and attractive for mass fabrication of periodic structures due to minimal chemical post-processing, high productivity and does not require expensive and energy consuming high-vacuum or ultraclean environments or special masks. By using this technique a rapid manufacturing of different periodic structures such as pillars, micro-tube or micro-lens arrays with different periods or more complex periodic micro-structures such as photonic crystals [13] or C-shape structures [14] is possible. Cheap micro-lens or micro-tube arrays are highly relevant in the modern technology for development of various integrated micro-optical or sensors systems and by management of fluid or gas flow at a microscopic level.

Another interesting topic for application of the periodic micro-structures is tissue engineering. The loss or failure of an organ or tissue is one of the most severe human health problems. Tissue or organ transplantation is a standard therapy to treat these patients, but this is severely limited by a donor shortage. Other available therapies to treat these patients - surgical reconstruction (e.g. heart), drug therapy (e.g. insulin for a malfunctioning pancreas), synthetic prostheses (e.g. polymeric vascular prostheses) and mechanical devices (e.g. kidney dialysers) - are not limited by supply, but they do not replace all functions of a lost organ or tissue and often fail in the long term. Tissue engineering has emerged as a promising approach to treat the loss or malfunction of a tissue or organ without the limitations of current therapies [15]. The major idea of tissue engineering is to create an artificial extracellular matrix (ECM) of biocompatible and biodegradable materials and seed on it the stem cells taken from the patient in order to produce a new tissue or organ, which can be transplanted back to the patient. The creation of artificial ECM imitating the natural extracellular matrix is a complex process that can be realized only by uniting knowledge of chemistry, biology, physics, engineering and materials sciences knowledge. In order to understand the cell behavior at the microscopic level it is important to create the highly reproducible micro-structures with easily controllable internal parameters. Interference lithography satisfies these criteria and in addition, the fabrication of periodic micro-structures by this technique is fast. However, for creation of artificial ECM close to natural extracellular matrix it is not enough to create a three-dimensional highly porous structure of

biodegradable and biocompatible material. It has long been recognized the importance of incorporating biomimetic signals within artificial matrices [16]. In natural tissues, cells recognize and attach to a specific amino acid sequences in extracellular-matrix protein molecules via integrins [17] which are activated by attaching ligands (molecules transmitting biosignals). The immobilization of ligands or other types of biomolecules in any desired place of artificial ECM would enable controlling the cell behavior. This idea can be realized by photo-grafting technique. Photo-grafting technique allows mimicking the ECM components and studying cell behavior – such as adhesion, spreading, migration, or differentiation – in response to the grafted molecules and patterns.

The scientific tasks of this work

The main aim of this work was to develop the formation technique of periodic micro-structures by interference lithography in photosensitive polymeric materials, experimentally investigate possibilities and limitations of the method, and to create micro-structures suitable for practical applications.

To achieve this aim, the following tasks were performed:

1. Estimate the limits of the geometrical properties of the periodic micro-structures fabricated by interference lithography, arising from the finite size of the experimental set-up;

2. Compare the efficiency of the micro-structures fabrication by the interference lithography with other photo-polymerization techniques: direct laser writing and optical vortex writing;

3. Investigate the influence of the laser processing parameters on the shape of the micro-structures fabricated by interference lithography;

4. Fabricate micro-structures by interference lithography in the larger area than the area of the beams overlapping;

5. Investigate the possibilities of the micro-structures photo-modification by photo-grafting technique.

Novelty and importance

For the first time, the possibility to form micro-tube arrays by using interference lithography was demonstrated and the control of the geometrical parameters of micro-lenses fabricated by interference lithography and manipulating the laser irradiation dose was investigated in depth. The possibility to immobilize the newly synthesized aromatic azides molecules in PEG matrix by photo-grafting technique was also demonstrated and the copper(I)-catalyzed azide–alkyne cycloaddition (CuAAC) chemical reaction by using azide "MegaStokes dye 673" was realized, in order to show the capability to combine the photo-grafting technique with "click" chemistry.

A part of the experiments made in this work have a practical value, since the interference lithography allows fast and effective fabrication of micro-structures suitable for different applications.

Statements to be defended

1. The shape of the micro-structures fabricated by interference lithography depends on the used laser irradiation dose, laser wavelength, phase, polarization, the angle between interfering beams and the number of the interfering beams, and their rigidity - mainly on the used laser irradiation dose.

2. The fabrication time of micro-tube array manufactured by interference lithography is lower compared to other methods based on the multi-photon polymerization: direct laser writing and optical vortex writing.

3. The top of the micro-pillars fabricated by the four-beam interference lithography and single-photon polymerization acquires the shape of the sphere part due to a different local degree of the cross-linking and shrinkage in the each central and side parts of the micro-pillars.

4. The fluoroaryl azides AFA and AFA-3 are immobilized on PEG-based matrix by two-photon absorption by using photo-grafting technique and 800 nm wavelength of the laser.

List of the author's publications related to thesis

1. **E. Stankevičius**, M. Gedvilas, B. Voisiat, M. Malinauskas and G. Račiukaitis, *Fabrication of periodic micro-structures by holographic lithography*, Lith. J. Phys., 53 (4), 227-237 (2013).

2. Z. Li, **E. Stankevičius**, A. Ajami, G. Račiukaitis, W. Husinsky, A. Ovsianikov, J. Stampfl and R. Liska, *3D alkyne–azide cycloaddition: spatiotemporally controlled by combination of aryl azide photochemistry and two-photon grafting*, Chem. Commun., 49, 7635-7637 (2013).

3. Z. Li, A. Ajami, **E. Stankevičius**, W. Husinsky, G. Račiukaitis, J. Stampfl, R. Liska, A. Ovsianikov, *3D photografting with aromatic azides: A comparison between three-photon and two-photon case*, Opt. Mater., 35 (10), 1846-1851 (2013).

4. **E. Stankevičius**, E. Balčiūnas, M. Malinauskas, G. Račiukaitis, D. Baltriukienė, V. Bukelskienė, *Holographic lithography for biomedical applications*, Proc. SPIE, 8433, 843312-7 (2012).

5. **E. Stankevičius**, T. Gertus, M. Rutkauskas, G. Račiukaitis, R. Gadonas, V. Smilgevičius and M. Malinauskas, *Fabrication of micro-tube arrays in photopolymer SZ2080 by using three different methods of direct laser polymerization technique*, J. of Micromech. Microeng., 22 (6), 065022 (2012).

6. M. Malinauskas, P. Danilevičius, E. Balčiūnas, S. Rekštytė, **E. Stankevičius**, D. Baltriukienė, V. Bukelskienė, G. Račiukaitis and R. Gadonas, *Applications of nonlinear laser nano/microlithography: fabrication from nanophotonic to biomedical components*, Proc. SPIE, 8204, 820407-2 (2011).

7. **E. Stankevičius**, M. Malinauskas, G. Račiukaitis, *Fabrication of scaffolds and micro-lenses array in a negative photopolymer SZ2080 by multi-photon polymerization and four – femtosecond – beam interference*, Physics Procedia, 12, 82-88 (2011).

8. **E. Stankevičius**, M. Malinauskas, M. Gedvilas, B. Voisat, G. Račiukaitis, *Fabrication of Periodic Micro-Structures by Multi-Photon Polymerization Using Femtosecond Laser and Four-Beam Interference*, ISSN 1392-1320 Mat. Sci. (Medžiagotyra), 17 (3), 244-248 (2011).

Others publications:

1. G. Račiukaitis, **E. Stankevičius**, P. Gečys, M. Gedvilas, C. Bischoff, E. Jäger, U. Umhofer, F. Völklein, *Laser processing by using diffractive optical laser beam shaping technique*, J. Laser Micro/Nanoeng., 6 (1), 37-43 (2011).

Summary of doctoral thesis

Doctoral thesis contains 7 chapters.
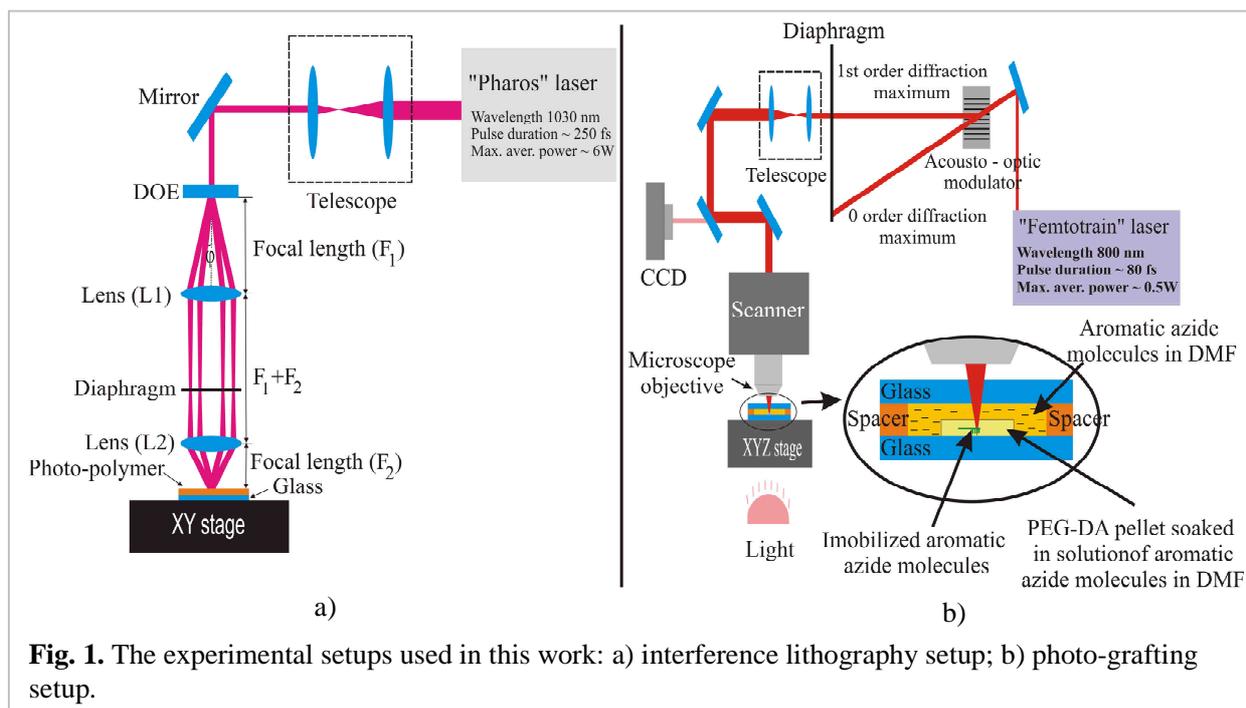
Chapter 1. Literature survey

In this chapter, the basics of the interference lithography and the photo-grafting techniques are reviewed. The interference phenomena and photo-polymerization principle are discussed. Other fabrication methods of periodic micro-structures such as direct laser writing based on photo-polymerization, UV lithography, soft lithography and stereo-lithography were reviewed. An overview of applications of periodic structures in such fields as photonics, micro-optics, micro-fluidics, thermoelectricity and tissue engineering was also provided.

Chapter 2. Materials and experimental techniques

Here, the experimental setups and materials used in this work are described and the limits of the smallest and largest periods of periodic micro-structures of the interference lithography experimental setup are discussed. The theoretical smallest period which can be fabricated by interference lithography is equal half of the used laser wavelength (diffraction limit).

In the experiments two different experimental setups were used (Fig. 1). In Fig. 1a the interference lithography experimental setup, which consists of a femtosecond Yb:KGW laser (Pharos, Light Conversion) generating ~ 250 fs pulses at 1030 nm (fundamental harmonic) and 515 nm (second harmonic) with the tunable repetition rate from 1 to 600 kHz and the maximum average power of ~ 6 W (fundamental harmonic) and ~ 3 W (second harmonic), a beam expander, a diffractive optical element (DOE) with 1.4 deg (fundamental harmonic) and 0.7 deg (second harmonic) separation angle between beams (Holo-Or Ltd.)

which splits the laser beam into four identical beams, diaphragm (D) which blocks undesirable higher order diffracted beams and two lenses (L1 and L2) system, is shown. Samples were mounted on an XY positioning system (Aerotech Inc.). The fabrication routine was controlled by the SCA software package (Altechna). The commercial hybrid organic-inorganic Zr-containing negative photoresist SZ2080 (chemical formula $C_4H_{12}SiZrO_2$) [18] (FORTH, Greece) with the photo-initiator 4,4'-bis(dimethylamino)-benzophenone (BIS) concentration by w. t. equal to 0.5% (in the second harmonic experiments) and 2% (in the fundamental harmonic experiments) was used. This material was chosen due to its low shrinkage, mechanical stability and possibility to photosensitize it optimally for the used irradiation. The theoretical smallest period of this experimental setup is approximately equal to the wavelength of the used laser (~ 515 nm – second harmonic and 1030 nm fundamental harmonic).

Fig. 1. The experimental setups used in this work: a) interference lithography setup; b) photo-grafting setup.

In Fig. 1b the photo-grafting experimental setup, which consists of a Ti:sapphire femtosecond laser (High Q, Femtotrain) emitting pulses with the duration of 80 fs at a 73 MHz repetition rate of around 793 nm, the 20x microscope objective (Zeiss, NA = 0.8) focusing the laser beam into the sample, an acousto-optical modulator used for fast switching of the laser beam and for adjusting its intensity, is shown. The photo-grafting

patterns were obtained by scanning the focused laser beam within the sample by the galvo-scanner (HurryScan, ScanLab). The CCD camera enabled online process monitoring. In photo-grafting experiments three types of aromatic azides molecules were used (Fig. 2).

Fig. 2. Aromatic azides molecules used in the photo-grafting experiments: a) BAC-M; b) AFA; c) AFA-3.

The samples in the photo-grafting experiments were prepared from poly(ethylene glycol) diacrylate (PEGDA, average M_n 700, Sigma Aldrich) and DMF mixture (ratio 50:50) with addition of 1 wt.% of the photo-initiator Irgacure819 (Ciba Specialty Chemicals Inc.). The resulting formulation was photo-polymerized with UV light for 5 min (Intelliray 600) in silicone molds (diameter 6 mm, thickness 1 mm). The photo-polymerized material pellets were soaked in DMF solution for at least 1 week, with the solvent being exchanged on a regular basis, in order to remove a residual monomer and a photo-initiator. For laser photo-grafting, the samples were immersed into the solution of BAC-M, AFA or AFA-3 in DMF.
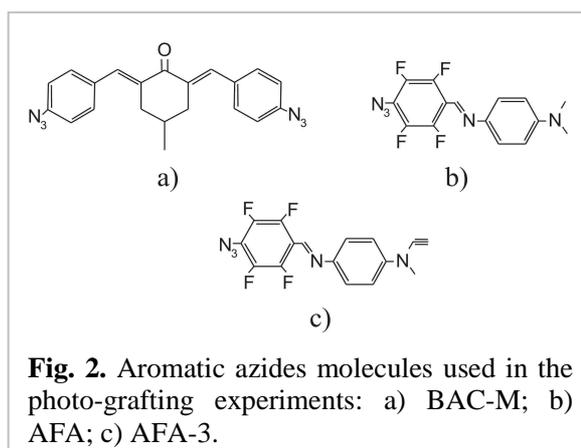
Chapter 3. The shape control of the micro-structures fabricated by interference lithography

In this chapter, the possibility to control the shape of micro-structures fabricated by interference lithography (IL) is described. The shape of fabricated periodic micro-structures by IL can be controlled by changing the angle between interfering beams and laser processing parameters (irradiation dose, used wavelength, phase and polarization of interfering beams).

The shape of structures fabricated by IL depends on the intensity distribution of the interference field. By using IL it is possible to fabricate only periodic structures. The period of structures fabricated by IL depends on the angle between interfering beams and the wavelength of used beams ($\sim\lambda/\sin\theta$).

By fabricating periodical structures besides their period, the shape of pillars and the free space between the pillars (for example cell growth) are also important. This space can be

controlled by using a different laser wavelength or managing the laser irradiation dose (the product of the exposure time and the average laser power).

Structures fabricated using different wavelengths (fundamental and second harmonics of the laser) are compared in Fig. 3. The structures fabricated by using the second harmonic (515 nm) have thicker pillars than by using the fundamental harmonic (1030 nm) (Fig.
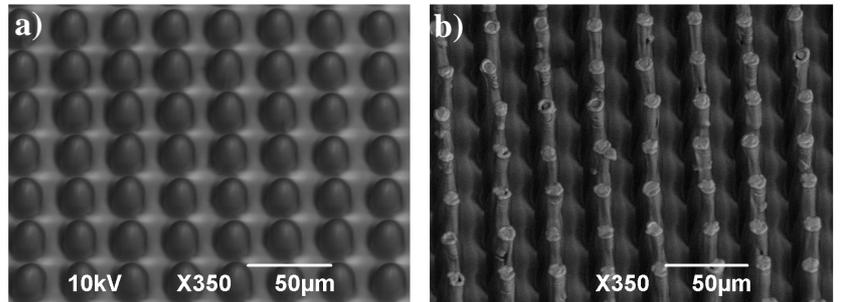

Fig. 3. Micro-structures fabricated in SZ2080 by using: a) the second harmonic (515 nm), the average laser power - 270 mW, the repetition rate - 100 kHz, the peak pulse intensity ~ 4.3 GW/cm^2, the exposure time - 5 s and BIS concentration of 0.5 % by w. t.; b) the fundamental harmonic (1030 nm), the average laser power - 700 mW, the repetition rate - 5 kHz, the peak pulse intensity ~ 0.22 TW/cm^2, exposure time - 5 min and BIS concentration of 2 % by w. t.. SEM images of the structures are tilted by 34 deg.

3) despite the fact that the laser irradiation was 155 times larger, the pulse energy was 51 times higher and the concentration of the photo-initiator was 4 times higher in experiments with the fundamental harmonic compared with the second harmonic. The reason for this effect is that the absorption of the used material (SZ2080 with photo-initiator 4,4'-bis(dimethylamino)benzophenone (BIS) in a solid state) at 515 nm (second laser harmonic) is about 20 % and at 1030 nm (fundamental harmonic) the used material is transparent. It means that by using the fundamental and second harmonics, the photo-polymerization process is initiated by different absorption mechanisms (single-photon – second harmonic, multi-photon – fundamental harmonic).

Micro-structures fabricated by the four-beam interference with a different exposure time by using the second harmonic (515 nm) and the same average power (~ 230 mW) are shown in Fig. 4. When the exposure time is too short (0.1 s) and the irradiation dose is close to the value where photo-polymerization process starts (photo-polymerization threshold), the fabricated structures are too weak and they do not survive the development process and collapse due to capillary forces (Fig. 4a) [19]. By increasing the laser irradiation dose, the photo-modification regions (blue area in Fig. 4) and the polymer chain length also increase

and the structures due to a higher cross-linking degree become stronger and they can survive the development process (Fig. 4b, the exposure time - 0.5 s). The increased laser irradiation dose initiates the photo-polymerization reactions over a larger area, and when photo-modified regions are close to each other, the radical diffusion from one photo-modified area to the other area starts. In this way the array of each other overlapping micro-pillars is fabricated (Fig. 4c).

The shape of the fabricated periodic structure can also be managed by changing the phase or the polarization of interfering beams. The theoretically calculated four-beam interference pattern when the phase of two opposite interfering beams is shifted by $3/8\pi$ in respect to the other two beams is shown in Fig. 5a. In Fig. 5b the structure fabricated by the interference lithography technique using the two-beam phase shift is depicted. This phase difference results in the

Fig. 4. Micro-structures fabricated in SZ2080 with BIS concentration of 0.5 % by w. t. by the four-beam interference technique with different laser exposure times: a) t_1=0.1 s; b) t_2=0.5 s; c) t_3=1 s. On the right side the cross-section of intensity distribution of the interference pattern is shown. The blue regions are photo-modified areas; the red solid line is the periodic laser intensity distribution; Th – the threshold of the polymerization; d – the diameter of photo-modified area; x – the transverse spatial coordinate; PΔt – the laser irradiation dose. The laser processing parameters of the fabricated structures on the right side are: 515 nm, ~ 230 mW, 100 kHz, ~ 33 GW/cm^2; the period of interference pattern - 2.5 μm. SEM images of the structures are tilted by 34 deg.

appearance of the additional intensity maxima. The maximum surrounded by four initial maxima is weaker, but its intensity is still sufficient to initiate the polymerization process. In addition to the weak maximum (small pillar), links between all pillars are polymerized, which makes the structure stable even when separated from a substrate (free-standing).

By adding the fifth central beam (zero order) to four identical symmetrically located beams, the interference intensity distribution pattern becomes three-dimensional [20]. The
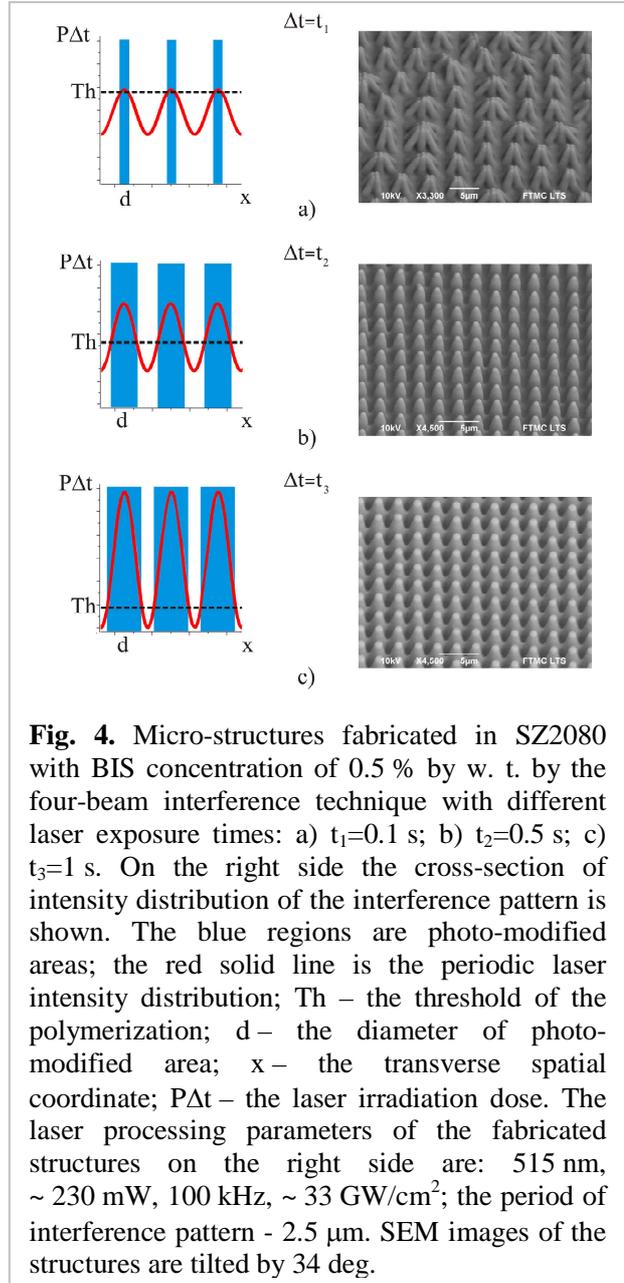
periodicity of this pattern in all directions depends on the angle between interfering beams [20]. When the angle between interfering beams is smaller than 10 deg, then the periodicity in z direction is more than 10 times larger than in x or y directions. By increasing the intensity of the fifth central beam, the modulation of every second interference maximum is also increasing (Fig. 6).
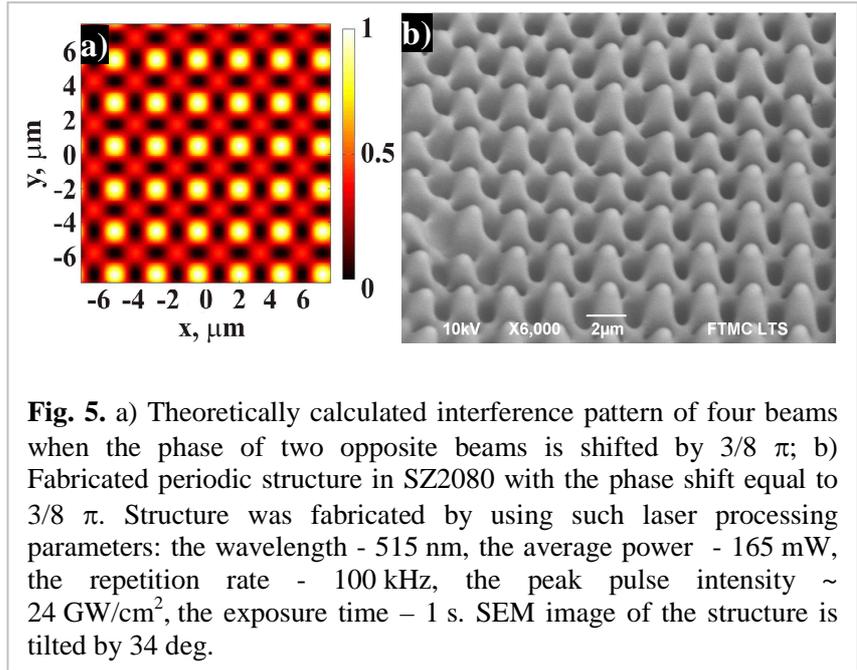

Fig. 5. a) Theoretically calculated interference pattern of four beams when the phase of two opposite beams is shifted by 3/8 π; b) Fabricated periodic structure in SZ2080 with the phase shift equal to 3/8 π. Structure was fabricated by using such laser processing parameters: the wavelength - 515 nm, the average power - 165 mW, the repetition rate - 100 kHz, the peak pulse intensity ~ 24 GW/cm^2, the exposure time – 1 s. SEM image of the structure is tilted by 34 deg.

The fabricated structures in SZ2080 photo-polymer with the five-beam interference pattern (Fig. 6) are shown in Fig. 7. The structures were fabricated with the same laser processing parameters only the thickness of the photo-polymer in this case was different: in Fig. 7a)
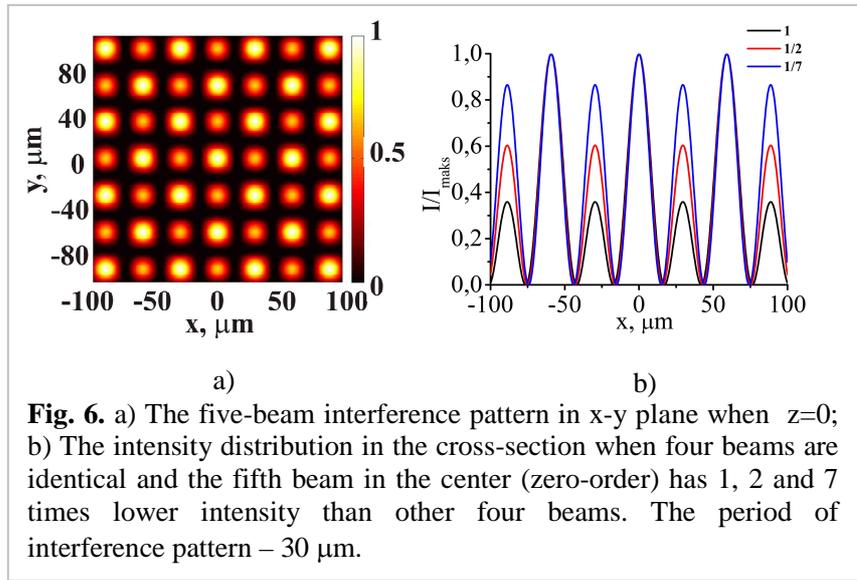

Fig. 6. a) The five-beam interference pattern in x-y plane when z=0; b) The intensity distribution in the cross-section when four beams are identical and the fifth beam in the center (zero-order) has 1, 2 and 7 times lower intensity than other four beams. The period of interference pattern – 30 μm.

~ 25 μm and in Fig. 7b) ~ 60 μm. As can be seen from Fig. 7 in this case the 2.5D structures were fabricated instead of 3D because the periodicity of a five-beam interference pattern in z direction under used experimental conditions (~ 3.45 mm) was larger than the thickness of the used photo-polymer. Since every second maximum of the used five-beam interference pattern is lower, the diameter of every second fabricated pillar is also smaller (Fig. 7a). The

pillars fabricated using the lower intensity in the thinner photo-polymer were strong enough to survive the development process and they were almost twice thinner than pillars fabricated using a higher intensity. The pillars fabricated using a lower intensity in the thicker
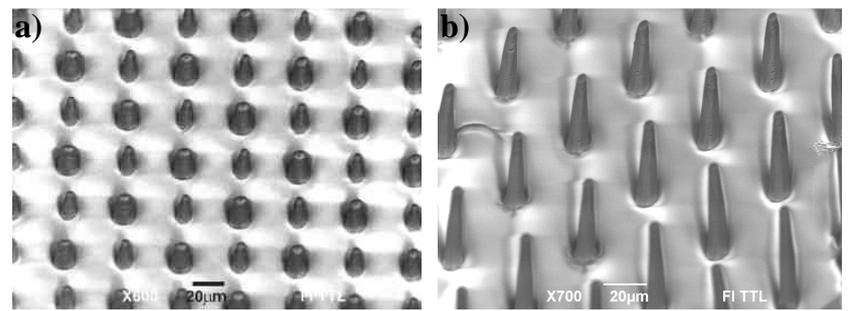

Fig. 7. Structures fabricated by the five beam interference pattern when four beams are identical and the fifth beam in the center (zero order) has 7 times lower intensity than other four beams with the average laser power of ~ 400 mW, the repetition rate - 5 kHz; the peak pulse intensity ~ 0.13 TW/cm^2; the photo-initiator BIS concentration of 2 % by w. t.; the exposure time - 25 s and the wavelength - 1030 nm at different thickness of photo-polymer: (a) ~ 25 μm, (b) ~ 60 μm. SEM images of the structures are tilted by 34 deg.

photo-polymer were not able to survive the development process and only pillars fabricated using a higher intensity remained. In this case the period of the fabricated structure is doubled without any intensity decrease in the beam overlapping area. In the normal way (by changing focal lengths of lenses), the intensity in the beam overlapping area decreases four times by increasing the period twice (by doubling the period). Therefore, the double-period effect can be used especially in the multi-photon polymerization process when high intensities are required.

Chapter 4. Fabrication of micro-tube arrays by interference lithography and comparison with direct laser writing and optical vortex writing methods

In this section, the fabrication of micro-tube arrays by using three different methods of direct laser polymerization techniques - direct laser writing (DLW), optical vortex writing (OVW) and interference lithography (IL) - is considered and compared.

Micro-tubes via DLW technique were fabricated by spiral scanning (step along z axis was 0.003 μm) with the laser beam of the Gaussian distribution in the photosensitive material (Fig. 8a). The intensity, applied to the fabrication of micro-tubes, was 0.85 TW/cm^2 and the sample translation velocity was equal to 1 mm/s. The example of the fabricated micro-tube array via DLW is depicted in Fig. 8b.
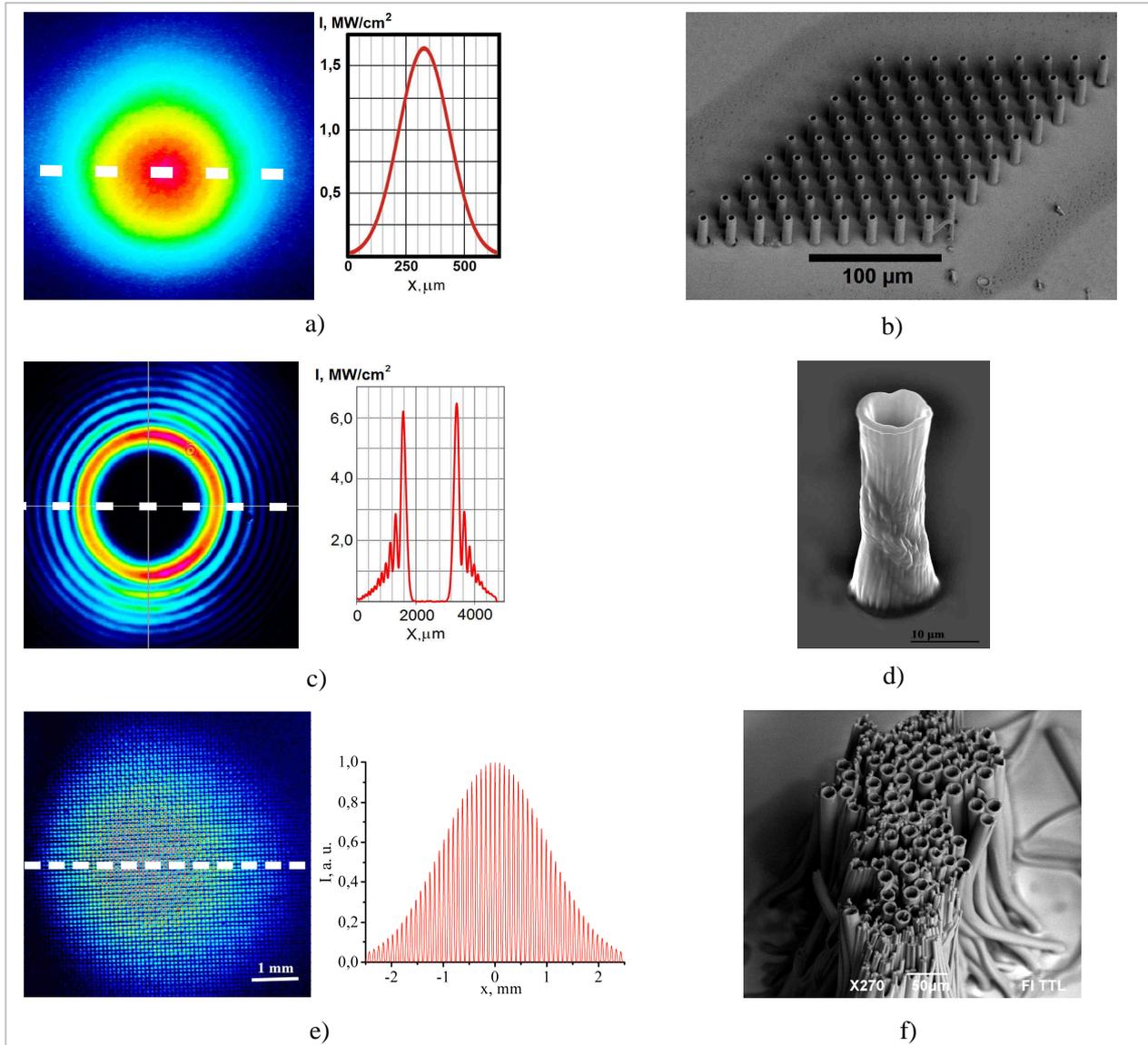
Fig. 8. a) On the left – the Gaussian beam intensity distribution used by the DLW technique; on the right – the Gaussian beam profile; b) Micro-tube array, fabricated using DLW method (tilted 34 deg). Laser pulse energy - 0.25 nJ, pulse repetition rate - 200 kHz; c) on the left – optical vortex beam (topological charge $m = 10$) intensity distribution; on the right – the vortex beam profile; d) SEM image of free standing micro-tube fabricated using the OVW method (tilted by 45 deg); e) on the left - intensity distribution as a product of the interference of four identical beams; on the right – calculated cross-section of intensity distribution of four identical beams interference in the interfering area; f) Micro-tube array fabricated using the IL method with the laser processing parameters: average power ~ 300 mW; pulse energy - 60 µJ; repetition rate – 5 kHz; exposure time - 1 min. SEM image of the structures is tilted by 34 deg.

Optical vortices for fabrication of micro-tubes were generated by using a S-waveplate which distorts the wavefront so that it becomes helical. Light intensity at the center of vortex is always zero and the phase is undefined. The intensity distribution in the generated

18

optical vortex beam with the topological charge $m = 10$ is shown in Fig. 8c. The aspheric lens $f = 6$ mm was used to focus the optical vortex beam. Intensity distribution in the focused optical vortex beam remains ring shaped. The size of the ring dark core depends on the topological charge. The laser pulse energy was chosen in such a way that only the inner ring had intensity above the photo-polymerization threshold.

Free standing micro-tubes inside the photosensitive material were fabricated by moving a focal plane of the optical vortex with the translation velocity of 1 mm/s in z direction only. The fabricated micro-tube is shown in Fig. 8d. The height of the micro-tube depended on the scanning distance along z axis. The surface roughness of the fabricated micro-tube was affected by the irregularity in the OVW beam intensity distribution and helical wavefront.

Array of micro-tubes was fabricated via interference lithography by recording the intensity distribution of four beams interference (Fig. 8e) and rotating the sample with a fixed radius using high energy pulses (~ 60 μJ). The example of micro-tubes fabricated by rotating the sample with radius of 10 μm and translation velocity of 1 mm/s is shown in Fig. 8f. The diameter of fabricated micro-tubes was 20 μm. It should be possible to form arrays of micro-tubes with a different diameter by choosing the radius of rotation.

Table 1. Comparison of the fabrication time between all three methods when the height of micro-tubes is 60 μm and the inner radius – 3 μm.

	Fabrication time of one single micro-tube, s	Fabrication time of micro-tube array containing 400 micro-tubes, s
DLW	30	~ 12012 (200 min)
OVW	0.06	~ 36
IL	0.075	~ 30

The comparison of the fabrication time between the three fabrication methods is shown in table 1. As seen from the table 1, the longest fabrication time of one micro-tube with the 60 μm height and the 3 μm inner radius is for the DLW method (30 s) and time by the OVW and IL methods is comparable, 0.06 s and 0.075 s, respectively. The OVW method allows fabrication of one single micro-tube with the 60 μm height and the 3 μm inner radius which is about 500 times faster than the DLW method and 1.25 times faster than by the IL method.

The fabrication time of one single micro-tube by the IL method was estimated despite the

fact that a micro-tube array by the IL method is fabricated by a single laser exposure. It means that the fabrication of a micro-tube array by the IL method does not take time for sample translation while in the DLW and OVW methods it is inevitable. Therefore, in the fabrication time of the micro-tube array by DLW and OVW methods sample translation time between two tubes should be estimated. In general the fabrication time of the micro-tube array by DLW and OVW methods can be expressed as:

$$t_{array} = M(t_{tube} + t_{translation}) \tag{1}$$

where t_{array} is the fabrication time of the micro-tube array by DLW or OVW method; M is the size of array; t_{tube} is the fabrication time of a single micro-tube by DLW or OVW method, $t_{translation}$ is the translation time between two micro-tubes.

When the translation velocity and period between micro-tubes are 1 mm/s and 30 μm and the size of the array is 400, the fabrication time of the micro-tube array by the OVW method increases by about 40 % due to the sample translation time. Then the IL method becomes more efficient than other methods. In this case the fabrication of the array containing 400 micro-tubes with the 60 μm height and the 3 μm inner radius by the IL method is 400 times faster than by DLW and 1.2 faster than by the OVW method. The time estimated for the fabrication of the 60 μm height and the 3 μm inner radius micro-tube array containing 400 micro-tubes by different methods is shown in table 1.

Chapter 5. The fabrication of micro-lens array by interference lithography

Here, rapid fabrication of the micro-lens array by interference lithography is presented and the possibility of their geometrical parameter control by changing the laser irradiation dose, the photo-polymer thickness and the period of intensity distribution is demonstrated.

By using four-beam interference pattern and thin photo-polymer thickness (< 20 μm) it is possible to fabricate micro-structures the form of which is similar to that of micro-lens (Fig. 9a). The fabricated micro-lenses demonstrate the focusing ability and the possibility of imaging objects (Fig. 9b). In Fig. 9b the image of the CPST logo pattern taken by the lenses manufactured by IL technique is shown.

The micro-pillars array formed by four beam interference lithography get the form of micro-lens due to several reasons:

1) the micro-pillars begin to grow

Fig. 9. a) Micro-lens array fabricated by interference lithography technique. Process parameters: laser wavelength – 515 nm, average laser power ~ 530 mW, repetition rate – 10 kHz, exposure time ~ 5 min. The distance between micro-lenses - 90 μm. SEM image of the structure is tilted by 34 deg.; b) Image of the CPST logo pattern taken by the lenses shown in a).

from the bottom despite the fact that the polymer chains are formed within the whole volume of the light affected photo-polymer (Fig. 10e). The observed experimental results allows us to make an assumption that the polymer chains unattached to the substrate are washed out by the development process;

2) the photo-polymerization rate of the polymer chains attached to the substrate is higher in the higher intensity area ($R_p \sim \sqrt{I}$) [21]. It means that the central part of micro-pillar is growing faster than the side parts and will grow taller;

Fig. 10. The principle of micro-lens formation process by IL technique: a) sample before laser processing; b) the sample irradiation by interference field; c) the initiation of radicals generation; d) polymer chain formation and radicals diffusion; e) polymer chain growth; f) fabricated micro-structure and their inner state; g) micro-lens formation due to the shrinkage of material and the gravity impact.

3) the central part of the micro-pillars is stronger than the side parts due to four-beam interference intensity distribution. In the central part of micro-pillars where a higher intensity was used the longer polymer chains were formed. In the side parts of the micro-pillars where a lower intensity was used the shorter polymer chains were formed (Fig. 10f).
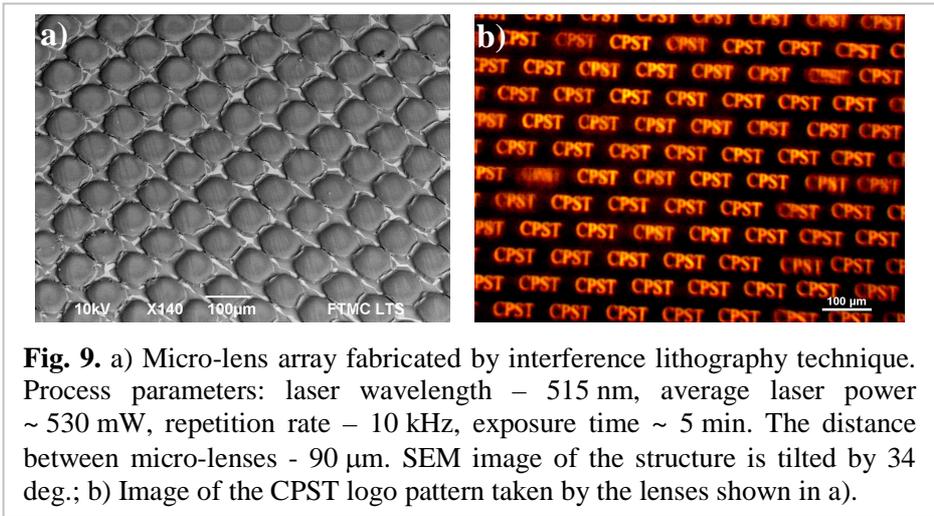
21

Longer polymer chains can get tangled up in each other more than shorter polymer chains. It means that they "stick" together better and form a greater number of chemical bonds with each other (have a higher cross-linking degree). A higher degree of cross-linking in the central part than in the sides parts of the micro-pillar determines the higher rigidity of the central part of the micro-pillar [19]. For this reason the side parts of the micro-pillar due to the gravity slump more than the central part;

4) After the development process micro-pillars start to shrink, the stronger part (central) of the micro-pillars shrinks less than weaker part (side) [22].

All the above mentioned reasons determine that the top of the micro-pillars fabricated by IL technique forms part of the sphere (Fig. 10g). The micro-lenses fabrication by IL was observed only in the case of the linear absorption. In non-linear absorption experiments the fabricated micro-pillars had sharp sides and their form was not similar to the shape of the micro-lenses.

The fabricated micro-lenses were characterized by using a scanning electron microscope (SEM) "JEOL JSM-6490LV", the surface profiler "Dektak 150+", an atomic force microscope (AFM) "Veeco Dimension Edge" and an optical microscope "Nikon Eclipse LV100". These devices allow the determination of the geometrical parameters (height, diameter and radius) of the fabricated micro-lenses, the evaluation of their surface roughness and the demonstration of the imaging possibilities. The measured surface roughness of fabricated micro-lenses is ~ 4 nm, it is less than $\lambda/10$ when $\lambda > 400$ nm. This value of the surface roughness is comparable with the surface quality of the micro-lenses fabricated by other methods [23].

The example of micro-lenses fabricated with a different laser irradiation dose is shown in Fig. 11. The micro-lenses depicted in Fig. 11 were fabricated by using the same exposure time (30 s) and a different average laser power (~ 470 mW, ~ 630 mW and ~ 930 mW). All micro-lenses depicted in SEM pictures were formed in the center of the interference area (where the intensity is highest).

As seen from Fig. 11 the micro-lenses shape can be managed by manipulating the laser irradiation dose during the lenses fabrication process.
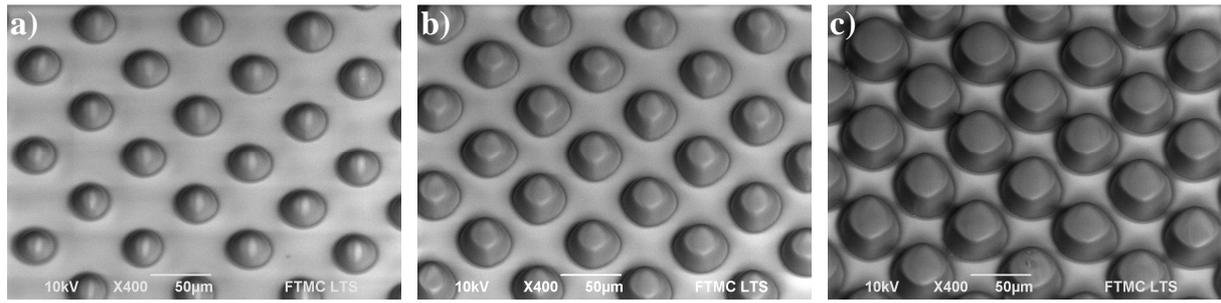
Fig. 11 Micro-lenses fabricated by interference lithography by using the same exposure time (30 s) and different laser average power: a) ~ 470 mW, b) ~ 630 mW and c) ~ 930 mW. The distance between micro-lenses is ~ 60 μm. Laser processing parameters are: wavelength - 515 nm, repetition rate - 100 kHz. SEM images of the structures are tilted by 34 deg.

The alteration of the micro-lenses diameter over the interference area by changing the laser irradiation dose is shown in Fig. 12. In x axis the number of micro-lenses fabricated by a single laser exposure is presented. The numbers for micro-lenses were given in such order: the micro-lens
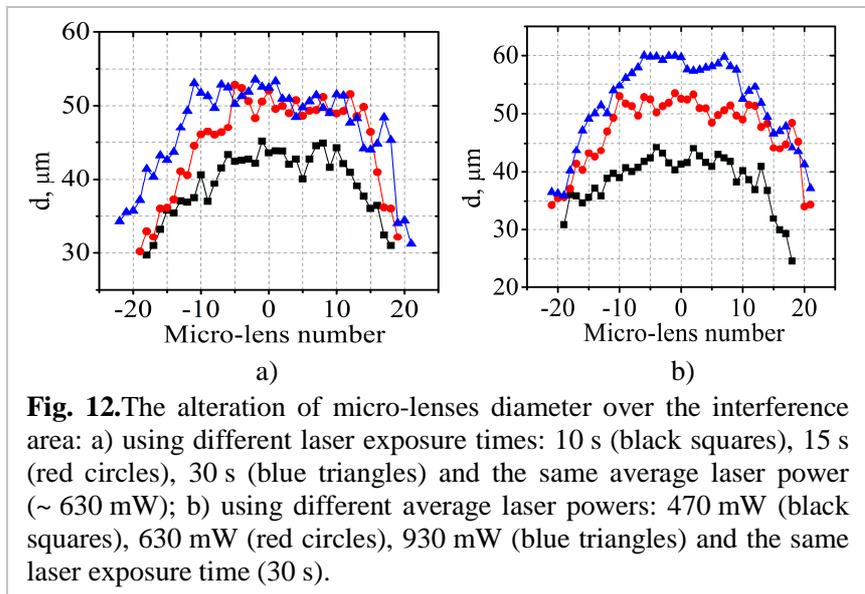

Fig. 12. The alteration of micro-lenses diameter over the interference area: a) using different laser exposure times: 10 s (black squares), 15 s (red circles), 30 s (blue triangles) and the same average laser power (~ 630 mW); b) using different average laser powers: 470 mW (black squares), 630 mW (red circles), 930 mW (blue triangles) and the same laser exposure time (30 s).

fabricated in the center of the interference area got number 0. To the left from this micro-lens, the numbers of micro-lenses were decreasing and to the right – increasing. Such numeration allows comparing the diameters of micro-lenses fabricated by a single laser exposure and a different laser irradiation dose because the count of micro-lenses fabricated by a different laser irradiation dose is different.

As seen from Fig. 12, the diameter of fabricated micro-lenses by a single laser exposure depends on both laser irradiation dose parameters: the laser exposure and the average laser power. It is also seen that the diameters of micro-lenses fabricated by a single laser exposure are not equal. The diameter of micro-lenses in the center of the interference area is larger than on the side of the area because the envelope of intensity distribution during the micro-lenses fabrication process in the interference area is Gaussian (Fig. 8e).

23

In Fig. 12a it is shown that the diameters of micro-lenses fabricated with exposure times of 15 s and 30 s are almost equal (the different is no more than 5 %). In this way the diameters of micro-lenses are saturated because all photo-initiators in the light affected area are activated and used in photo-polymerization process. It means that no more new radicals are generated even if the light is still irradiating the sample. The diameter of micro-lenses can still slightly increased by using higher-energy pulses (Fig. 12b) but it can not be larger than the period of interference intensity distribution.

The diameter of micro-lenses fabricated by interference lithography depends on the density of radicals generated during the laser exposure. The density of radicals ρ generated by femtosecond laser pulses in a single photon absorption case by analogy with two-photon absorption [3] can be calculated by solving a simple rate equation:

$$\frac{\partial \rho}{\partial t} = (\rho_0 - \rho)\sigma_1 N \qquad (2)$$

where ρ - is the density of radicals, t - is time, ρ_0 - is the primary initiator particle density, σ_1 - is the effective single-photon cross-section for the generation of radicals, N - is the photon flux.

In eq. (2) the diffusion of the generated radicals and their loss due to reactions with oxygen or others radicals are not taken into account.

The absorbed power into a volume unit can be written:

$$q = -\frac{\mathrm{d}I}{\mathrm{d}z} = \alpha I \qquad (3)$$

where q – is the absorbed irradiation into a volume unit, I – is the laser intensity, z – is the longitudinal coordinate, α – is the linear absorption coefficient.

In the linear absorption case it is possible to calculate the intensity of the transmitted light through the sample as eq. (3) with boundary condition $I(z=0) = I_{z=0}$ has a solution, known as the Beer-Lambert law:

$$I(z) = I_{z=0}e^{-\alpha z} \qquad (4)$$

here $I_{z=0}$ – is the value of the intensity of the incident irradiation.

For low absorbing material $e^{-\delta} \approx 1 - \delta$, $\delta << 1$, then eq. (4) can be rewritten:

$$I(z) = I_{z=0}e^{-\alpha z} \approx I_{z=0}(1 - \alpha z) \tag{5}$$

The transmission spectrum at 515 nm wavelength (second harmonic of the used laser) of the material SZ2080 (used in the micro-lens fabrication) is about 80 % when the thickness of the sample - 1 mm. It means that the coefficient of the materials absorption $\alpha = -1/z \ln T = 2.2 \text{ cm}^{-1}$. Since in micro-lens formation experiments the thickness of the sample was ~ 20 μm or $\alpha z \approx 0.0044 \ll 1$, then it was possible to use eq. (5). It means that the power absorbed into the volume unit does not fluctuate in all the thickness of the sample and depends only on the transverse coordinate:

$$q(x) = \alpha I(x) \tag{6}$$

It is logical to assume that the energy density is proportional to the absorbed photon flow multiplied by the effective single-photon cross-section for the generation of radicals:

$$q \propto \sigma_1 N \tag{7}$$

Then, by using (6) and (7) equations, radical growth eq. (2) can be rewritten as follows:

$$\frac{\partial \rho(x)}{\partial t} = \alpha (\rho_0 - \rho(x)) I(x) \tag{8}$$

This differential equation has a solution, which describes the density of radicals generated at some moment of the laser irradiation:

$$\rho(x) = \rho_0 \left[1 - \exp(-\alpha I(x) \tau_p f_{rep} t) \right] \tag{9}$$

here τ_p – is the laser pulse duration, f_{rep} – is the laser repetition rate, t – is the exposure time.

The photon flux modulated in the space in a four-beam interference case can be written:

$$I(x) = I_0 \cos^4 \left(\frac{\pi}{\sqrt{2}\Lambda} x \right) \tag{10}$$

here $I(x)$ - is intensity distribution function in a four-beam interference case, I_0 - is the peak intensity of the interference maximum, x - is the transverse coordinate, Λ - is the period of the interference intensity modulation.

By inserting eq. (10) into eq. (9), the fluctuation of radicals density initiated by four beam interference at the some moment t of the laser irradiation can be expressed as:

$$\rho(x) = \rho_0 \left[1 - \exp\left(-\alpha I_0 \cos^4 \left(\frac{\pi}{\sqrt{2}\Lambda} x \right) \tau_p f_{rep} t \right) \right] \tag{11}$$

Since the resin is polymerized as soon as the particle density of radicals ρ exceeds a certain minimum concentration (threshold value) $\rho_{th.}$, hence it is possible to make an assumption that the diameter of micro-lens fabricated by interference lithography (d) is equal to an area where the density of radicals exceeds the threshold of the polymerization ($\rho(x)=\rho_{th}$) and can be expressed as:

$$d = \frac{2\sqrt{2}\Lambda}{\pi}\arccos\left[\left(\frac{C}{I_0 t}\right)^{\frac{1}{4}}\right] \qquad (12)$$

where $C = \frac{1}{\alpha\tau_p f_{rep}}\ln\left(\frac{\rho_0}{\rho_0 - \rho_{th}}\right)$.

Eq. (12) theoretically describes the dependence of the diameter of micro-lenses fabricated by four-beam interference lithography on the peak intensity of the interference maximum and the laser exposure time.

The theoretically calculated dependence of the micro-lens diameter by eq. (12) on the peak interference maximum intensity with different exposure times fits to the experimentally measured micro-lens diameters values (Fig. 13a).

Fig. 13. The dependence of the micro-lens diameter (a) and height (b) on the peak interference maximum intensity by using different laser exposure times: 10 s (black), 15 s (red), 30 s (blue): theoretically calculated (lines) and measured (points).

The laser irradiation dose influences not only the diameter of fabricated micro-lenses but the height as well. The alteration of the micro-lenses height over the interference area by changing the laser irradiation dose is shown in Fig. 14. The numeration of the micro-lenses in Fig. 14 is the same as in Fig. 12.

As seen from Fig. 14, the height of micro-lenses in the central part of the interference area is higher than in the side part of the interference area (due to higher intensity in the central part). The height of fabricated micro-lenses is increasing by increasing the laser
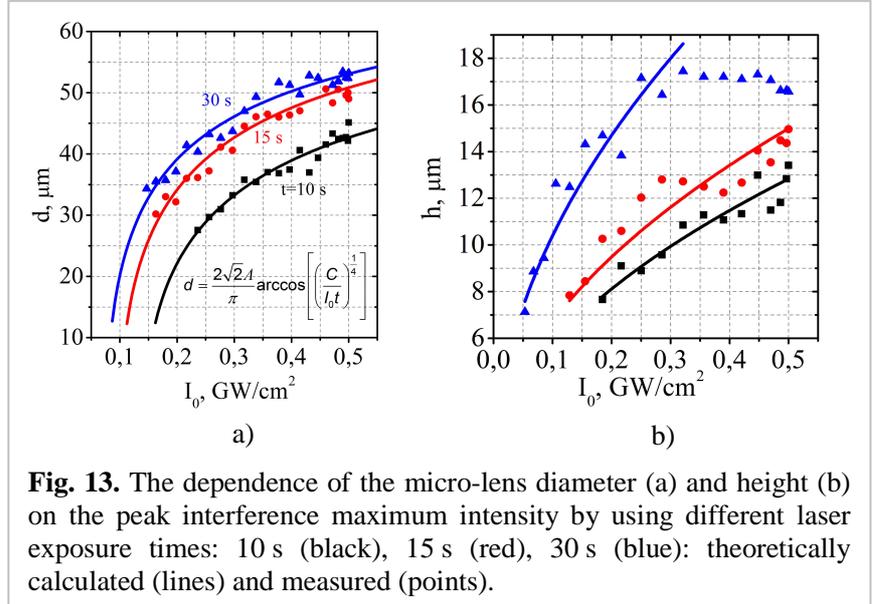
exposure time (Fig. 14a) or the average laser power (Fig. 14b).

When the laser irradiation dose is high (in our case the exposure time of 30 s and the average laser power of 630 mW or 930 mW), the he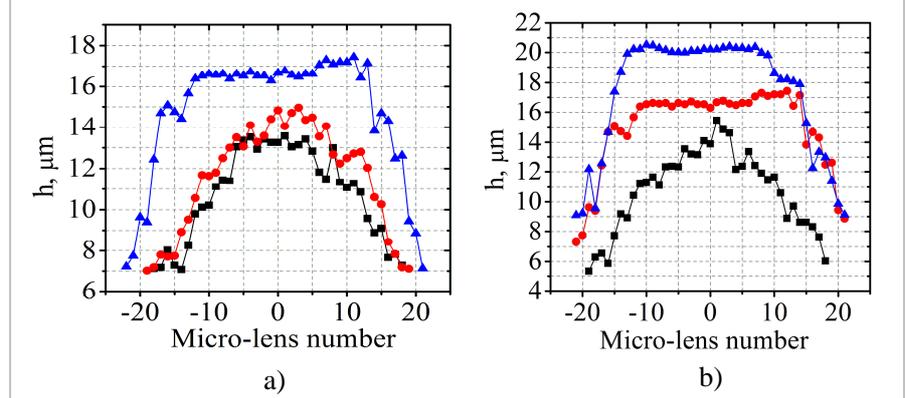ight of micro-lenses reaches the saturation in the central part of the interference area. The saturation of the micro-lenses height is determined by the photo-polymer thickness, the radical diffusion and the polymerization rate.

Fig. 14. The alteration of micro-lenses height over the interference area: a) using different laser exposure times: 10 s (black squares), 15 s (red circles), 30 s (blue triangles) and the same average laser power (~ 630 mW); b) using different average laser powers: 470 mW (black squares), 630 mW (red circles), 930 mW (blue triangles) and the same laser exposure time (30 s).

The dependence of the micro-lens height on the peak interference maximum intensity with different exposure times is shown in Fig. 13b. As seen from Fig. 13b, the height of micro-lenses is proportional to the square of the peak intensity ($h \sim \sqrt{I_0}$). It is means that the growth of micro-lenses determines the polymerization rate (R_p) because it is also proportional to the square of the peak intensity [21]:

$$R_p = \frac{k_p}{\sqrt{2k_t}} \sqrt{\Phi \sigma [A] I \tau_p \nu / \left[2(\hbar \omega)^2 \right]} \qquad (13)$$

where k_p - is the rate constant for chain reaction propagation, k_t - is the rate constant for chain reaction termination Φ - is the quantum yield for radical generation, i.e., the probability that an excited photo-initiator will give rise to a radical, σ - is the single photon cross section of the initiator, $[A]$ - is the concentration of the photo-initiator, $\hbar \omega$ - is the photon energy, I - is the light intensity, τ_p - is the pulse duration, ν - is the laser repetition rate.

Since the micro-lens array in the experiments was fabricated by a single laser exposure and in the same sample, so it means that only one parameter describing the polymerization

27

rate was varying during the fabrication process - the peak pulse intensity of the interference maximum. Hence, it is possible to make the assumption that the height of micro-lenses fabricated by interference lithography is proportional to the polymerization rate ($R_p \sim \sqrt{I_0}$).

One of the most important parameter of micro-lenses is a radius of curvature. This parameter can be controlled by manipulating the laser irradiation dose. The alteration of the micro-lenses radius of curvature over the interference area by changing the laser irradiation dose is shown in Fig. 15.

As seen from Fig. 15, when the laser exposure time is shorter (10 s or 15 s) and the average laser power is lower (~ 470 mW), the radius of curvature is between 20 μm and 30 μm and it is almost equal in all the interference area. When the laser exposure time
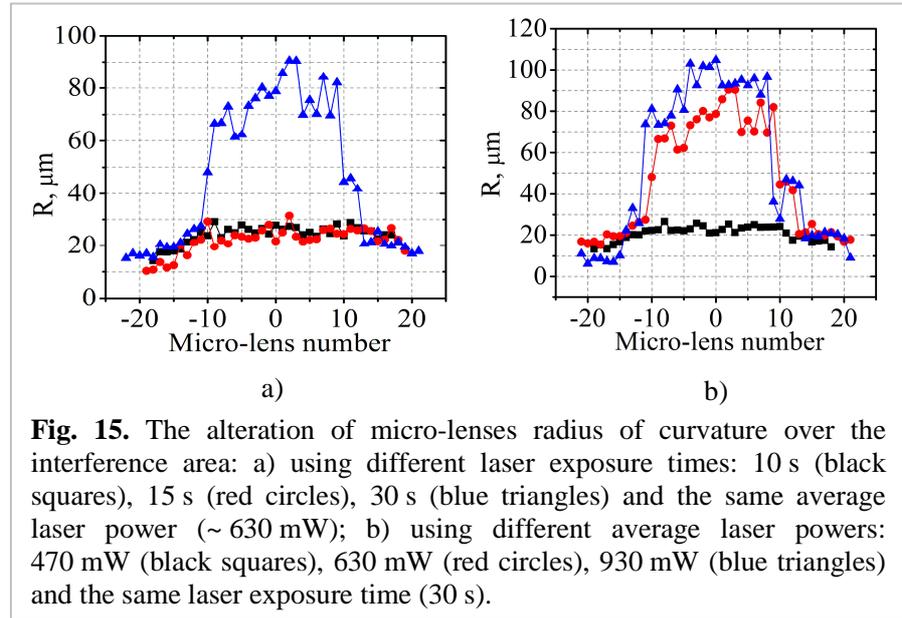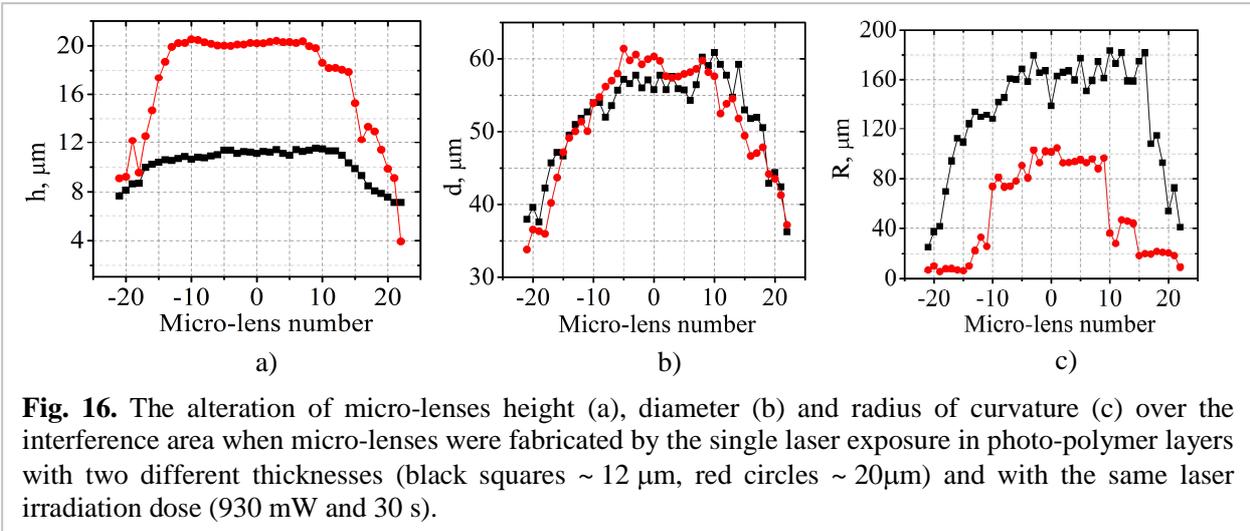

a)   b)

Fig. 15. The alteration of micro-lenses radius of curvature over the interference area: a) using different laser exposure times: 10 s (black squares), 15 s (red circles), 30 s (blue triangles) and the same average laser power (~ 630 mW); b) using different average laser powers: 470 mW (black squares), 630 mW (red circles), 930 mW (blue triangles) and the same laser exposure time (30 s).

is 30 s and the average laser power ~ 630 mW or ~ 930 mW, the radius of curvature of micro-lens is increasing 5 times in the central part of the interference area. This increase is related to the saturation of the height of the micro-lens.

The shape of micro-lenses can also be controlled by using a different thickness of the photo-polymer. The geometrical parameters of fabricated micro-lenses in the different photo-polymer thickness are presented in Fig. 16. As seen from Fig. 16 the diameters of fabricated micro-lenses are equal and only the heights are different and they depend on the thickness of the photo-polymer. The curvature of a radius is larger for the micro-lenses fabricated in the thinner layer of the photo-polymer.

Another opportunity to manage the geometrical parameters of micro-lenses during the fabrication process by interference lithography is to use a different period of the interference

intensity distribution.

Fig. 16. The alteration of micro-lenses height (a), diameter (b) and radius of curvature (c) over the interference area when micro-lenses were fabricated by the single laser exposure in photo-polymer layers with two different thicknesses (black squares ~ 12 μm, red circles ~ 20μm) and with the same laser irradiation dose (930 mW and 30 s).

Chapter 6. The fabrication of scaffolds by interference lithography

In this chapter, the scaffolds fabricated from diacrylated poly(ethylene glycol) (PEG-DA-258) over a large area by interference lithography technique are presented. The example of fabricated scaffold by IL is shown in Fig. 17a.

A rabbit myogenic stem cells suspension was prepared and seeded onto each prepared PEG-DA-258 scaffold. The PEG-DA scaffolds fabricated by interference lith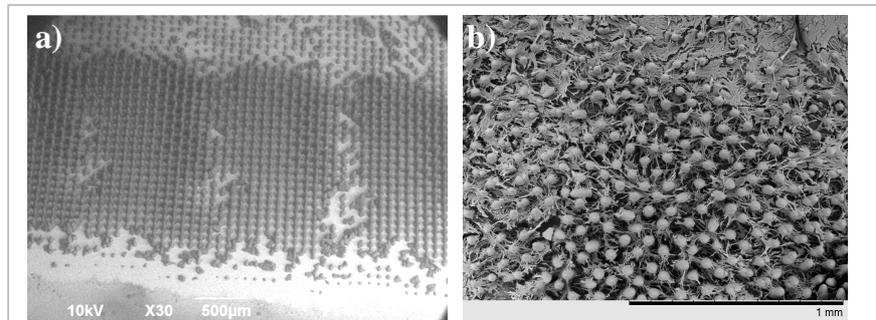ography showed good cyto-compatibility for rabbit myogenic stem cells. It was observed that adult rabbit muscle-derived myogenic stem cells

Fig. 17. a) Stitched area of micro-structures fabricated from PEG-DA-258 by IL with the exposure time of 15 s and the average laser power ~ 540 mW (peak pulse intensity ~ 13 GW/cm^2, laser dose ~ 8.1 J); b) SEM images of structures fabricated from PEG-DA-258 with rabbit myogenic stem cells grown for four days.

grew onto PEG-DA scaffolds (Fig. 17b). They were attached to the pillars and formed cell-cell interactions. It demonstrates that the fabricated structures have potential to be an interconnection channel network for cell-to-cell interactions, flow transport of nutrients and metabolic waste as well as vascular capillary in-growth. Apart from the fundamental

requirements of an adequate pore size, surface charge, roughness, hydrophobicity, etc., pore interconnectivity also plays a key role in the cells interaction with scaffolds. Insufficient interconnectivity in biodegradable hydrophobic polymers has been shown as a limiting factor in cell colonization and new tissue formation [24].

In our study it has been observed that the proliferation of the rabbit myogenic stem cells depends on the period of the fabricated PEG-DA-258 scaffold. From Fig. 18 it was observed that the larger number of stem
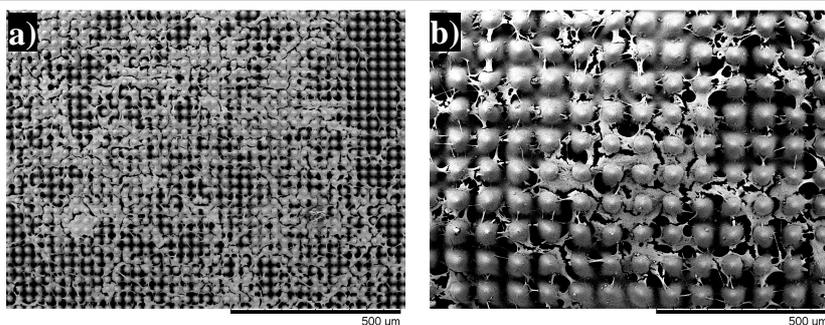

Fig. 18. SEM images of scaffolds fabricated from PEG-DA-258 with rabbit myogenic stem cells grown for two days: a) period 30 μm; b) period 90 μm.
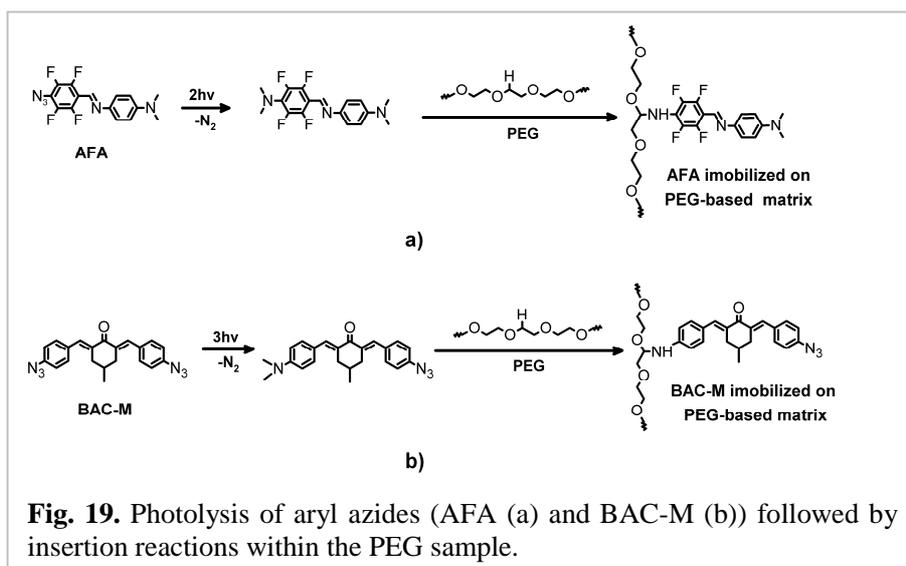
cells was on the scaffolds with a smaller period. These results can be explained so that the space between the pillars of scaffolds with a smaller period is smaller than the cells size (from 20 μm to 60 μm) and it allows the cells to attach the pillars of the scaffolds more easily.

Chapter 7. Photo-modification of the polymeric structures by photo-grafting technique

Here, novel fluoroaryl azides photo-grafting compounds (AFA and AFA-3) were synthesized and their processing windows and spatial resolutions of immobilization on a PEG-based matrix were compared with the commercially available azide BAC-M. The ability of the immobilized AFA-3 molecule to join dye-functionalized molecules containing "clickable" azide moieties via CuAAC "click" chemical reaction was also demonstrated.

Chemical reactions of an immobilization process of AFA and AFA-3 molecules on PEG based matrix by photo-grafting process are shown in Fig. 19a and Fig. 22a. These chemical reactions are analogous to the chemical reactions of BAC-M photo-grafting process on PEG based matrix (Fig. 19b). As seen from these chemical reactions, the focused laser beam

induces photolysis of the azides which causes the dissociation of the N–N bond from the excited singlet state, followed by the generation of nitrogen and highly reactive electron-deficient nitrene species. The short-lived

Fig. 19. Photolysis of aryl azides (AFA (a) and BAC-M (b)) followed by insertion reactions within the PEG sample.
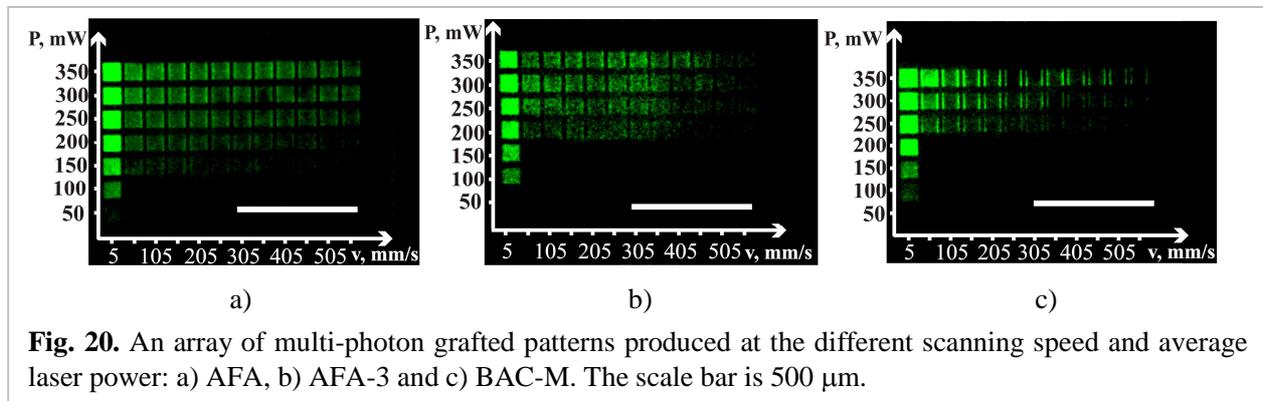
nitrene intermediate is directly immobilized on the PEG network by insertion into a C–H bond. This single-step process is universal, since it is applicable to a wide variety of matrices containing C–H or N–H bonds.
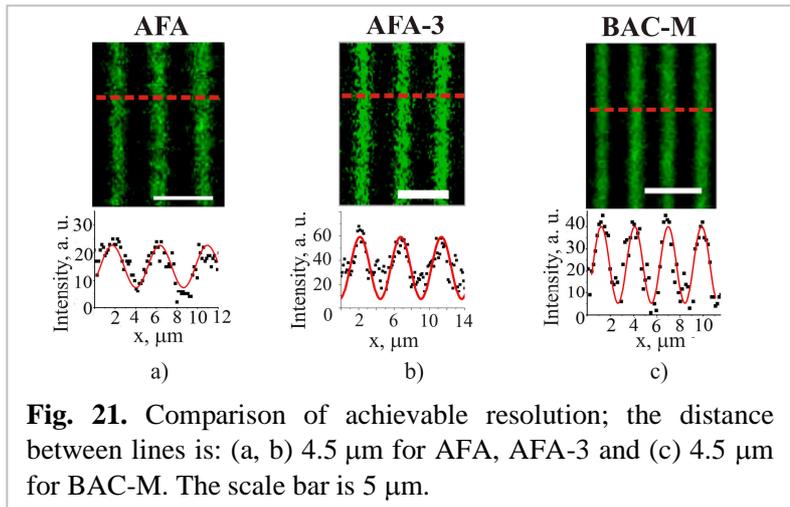
The grafted patterns were produced by a set of adjacent line scans at a distance of 1.5 μm with a different average laser power (50 mW - 350 mW, step 50 mW) and scanning velocity (5 mm/s – 555 mm/s, step 50 mm/s). In the vertical direction a step of 5 μm (total 7 slices) was used. After the grafting procedure, the samples were placed in DMF in order to remove the residual BAC-M, AFA or AFA-3 molecules. Rapid decoloration of the pellet indicated the successful removal of possible residuals from the sample. The fluorescence of the patterned samples was analyzed by laser scanning microscopy (LSM700 ZEN software, Carl-Zeiss) at the excitation wavelength of 555 nm.

The results of the experiments of the processing windows of the aromatic azides immobilization are shown in Fig. 20. As seen from Fig. 20, the immobilization processing window of AFA is broader than that of AFA-3 or BAC-M. It means that the AFA molecule can be photo-grafted on PEG-based matrix with a lower intensity and at a higher writing speed. The reason for it is that AFA has the highest absorption at the 800 nm wavelength. The photo-grafting process for AFA and AFA-3 molecules is initiated via two-photon absorption and for BAC-M - via three-photon absorption. However, the observed fluorescence intensities of grafted patterns of BAC-M at high laser intensities and a low

31

scanning speed are higher than those of AFA with the identical parameters. This difference can be explained by the photo-grafting products of BAC-M, which contain the ketocyanine chromophore with strong fluorescence [25]. It should be noted that the levels of immobilization can be spatially controlled by simply altering the irradiation exposure time or laser intensity during the photo-patterning process, as demonstrated in Fig. 20. Such controlled 3D spatial gradients cannot be generated by conventional photo-lithographic methods. The ability to produce biochemical and biomechanical gradients in 3D is important to numerous biotechnology applications [26].

Fig. 20. An array of multi-photon grafted patterns produced at the different scanning speed and average laser power: a) AFA, b) AFA-3 and c) BAC-M. The scale bar is 500 μm.

The achievable resolution for AFA, AFA-3 and BAC-M patterns produced with fixed grafting parameters (the average laser power of 350 mW and laser scanning speed of 5 mm/s) and molar concentration of azides molecules (14 mmol/L) was also compared (Fig. 21). It

Fig. 21. Comparison of achievable resolution; the distance between lines is: (a, b) 4.5 μm for AFA, AFA-3 and (c) 4.5 μm for BAC-M. The scale bar is 5 μm.

was evaluated that the width of single lines produced by using the above mentioned laser power and scanning parameters was around 2.5 μm for BAC-M and around 4.1 μm and 3.6 μm for AFA and AFA-3, respectively. The resolvability of lines is confirmed by the corresponding fluorescence intensity distribution. At a smaller distance the separate lines could not be distinguished. BAC-M shows a better spatial resolution than AFA or AFA-3.

32

Since the immobilization of the BAC-M molecule proceeds via 3PA process and of AFA and AFA-3 via 2PA process, the initial activation volume is expected to be smaller for BAC-M.

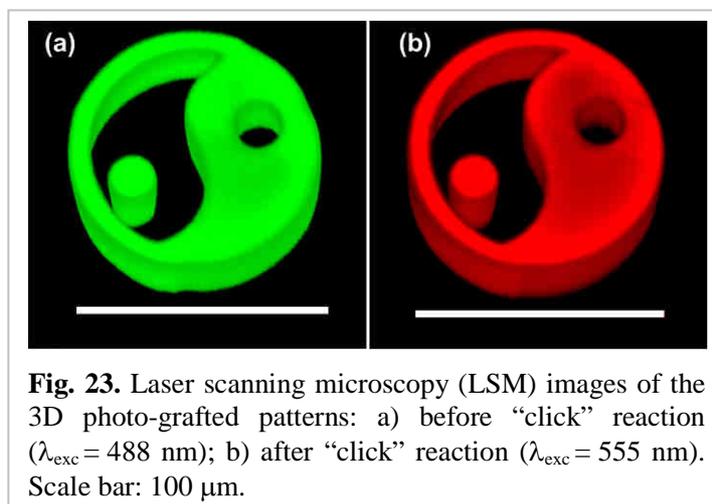Here, a strategy to realize spatio-temporal control of the CuAAC reaction in 3D was also reported (Fig. 22). The fluoroaryl azide with alkyne functionality was initially immobilized precisely within the PEG-matrix

Fig. 22. a) Two-photon absorption induced decomposition and subsequent insertion of AFA-3 into a PEG matrix, followed by CuAAC "click" reaction for post-modification; (b) schematic representation of the 2PA grafting procedure and post-modification.
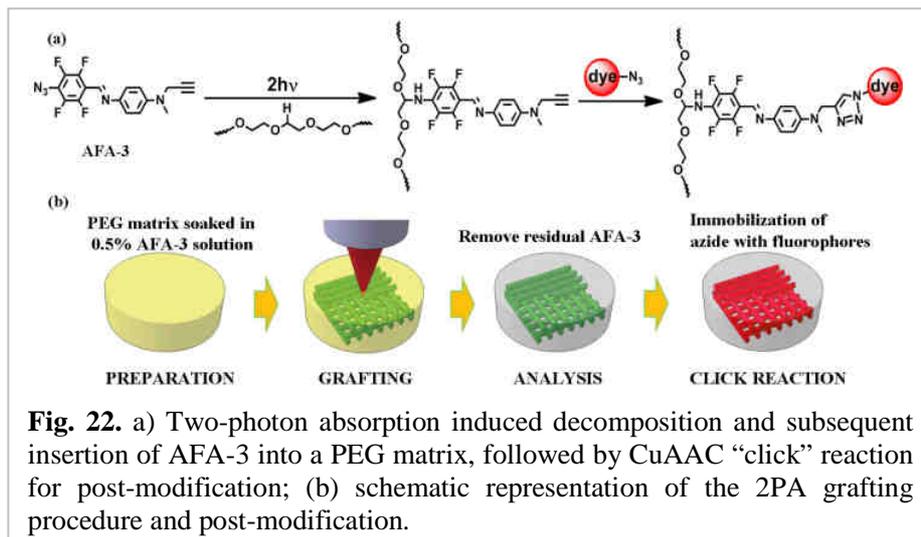
via photo-grafting. The covalently attached alkyne moieties served as anchors and subsequently reacted with functionalized molecules containing azide moieties via CuAAC "click" reaction.

Due to the distinct characters of the CuAAC "click" reactions, various functionalized molecules with azide moiety could be conjugated onto the formed "clickable" patterns containing alkyne functionalities produced by photo-grafting. Azide MegaStokes dye 673 was selected as a model precursor for the "click" reaction

Fig. 23. Laser scanning microscopy (LSM) images of the 3D photo-grafted patterns: a) before "click" reaction ($\lambda_{exc} = 488$ nm); b) after "click" reaction ($\lambda_{exc} = 555$ nm). Scale bar: 100 μm.

because the strong fluorescence emission of the dye is located at a long wavelength of 673 nm, at which the fluorescence of the "clickable" patterns produced by photo-grafting could not be observed. Therefore, an excellent differentiation of the fluorescent patterns before (Fig. 23a) and after "click" reaction could be achieved. The bright red fluorescence of the

pattern (Fig. 23b) indicates the successful 3D site-specific immobilization of the azide-fluorophores via CuAAC "click" reaction.

The developed 3D site-specific functionalization method is simple and versatile; it has potential applications in micro-array based proteome analysis, studies of cell-surface interactions, sensing applications, and drug screening.

Conclusions

1. The geometrical parameters and rigidity of the micro-structures fabricated by interference lithography can be controlled by manipulating the laser irradiation dose, the wavelength, the phase and the number of the interfering beams. The micro-pillars fabricated by interference lithography are stronger in the central part than in the side part of the interference zone as the intensity distribution during the fabrication process in the interference area is Gaussian. The micro-pillars fabricated in the side part of the interference area often collapse due to smaller rigidity and resultant capillary forces acting during the development process.

2. The periodic micro-structures fabricated by a single laser exposure can be extended over a larger area than the interference zone by selecting the appropriate laser processing parameters and the overlapping step between interference zones.

3. The fabrication rate of the micro-tubes array is the highest for the interference lithography compared to the others lithography techniques based on multi-photon polymerization: direct laser writing and optical vortex writing since the micro-tubes array is fabricated by the single laser exposure in the interference lithography case.

4. The fabrication of micro-tubes by direct laser writing technique demonstrates the best quality and reproducibility compared with interference lithography and optical vortex writing methods but the fabrication rate in this case is the lowest.

5. The top of the micro-pillars fabricated by the four-beam interference lithography and the single-photon polymerization takes the shape of the part of the sphere due to a different local degree of the cross-linking and shrinkage in the each central and side parts of the micro-pillars. Such micro-pillars (micro-lenses) can perform the objects imaging and

their surface roughness satisfies the requirements of the surface quality of the optical elements.

6. The fabrication of micro-lenses by interference lithography is a flexible approach which allows the possibility to control the geometrical parameters (diameter, height and curvature of radius) of the micro-lenses during the fabrication process by changing the laser irradiation dose, the photo-polymer thickness and the period of intensity distribution.

7. PEG-DA-258 scaffolds fabricated by interference lithography supporting rabbit myogenic stem cells growth. SEM images of pillar structures with myogenic cells after 4 days of culture revealed that the cells had attached to the PEG-DA-258 surfaces and penetrated into the interior of the scaffold. Furthermore, fabricated PEG-DA258 demonstrates low or no cytotoxicity and good cytocompatibility. It is possible to control the proliferation of cells on fabricated PEG-DA-258 scaffolds by manipulating the periodicity of scaffolds. The rabbit myogenic stem cells were growing better on the scaffolds whose period is close to the size of the cultivated cells.

8. Comparison of the AFA, AFA-3 and BAC-M has demonstrated that the intensity required to induce multi-photon absorption in AFA is a lower than for AFA or BAC-M. As a consequence, the AFA exhibits the largest processing window and supports a higher writing speed in photo-grafting process. However, due to the three-photon interaction nature, the volume in which BAC-M molecules are excited can be more confined. This is the advantage of BAC-M over AFA and AFA-3 since it leads to higher patterning resolution in multi-photon photo-grafting. The evaluated width of single lines produced by using the average laser power of ~ 350 mW, the scanning speed of 5 mm/s and 20x microscope objective (NA=0.8) is around 2.5 μm for BAC-M and around 4.1 μm and 3.6 μm for AFA and AFA-3, respectively.

9. By using the AFA-3 molecule it is possible to realize the 3D CuAAC „click" reaction via combination of arylazide photochemistry and two-photon grafting. 3D CuAAC "click" reaction was confirmed by the localized conjugation of the azide-fluorophores (characterized by a strong fluorescence emission at the wavelength of 673 nm) onto the

"clickable" covalently attached alkyne moieties. The presented strategy to realize 3D alkyne–azide cycloaddition with a highly spatiotemporal control is simple and versatile, which reveals great potential applications in micro-array based proteome analysis, biosensors, cell patterning, and drug screening.

References

[1]   T. Kondo, S. Matsuo, S. Juodkazis and H. Misawa, *"Femtosecond laser interference technique with diffractive beam splitter for fabrication of three-dimensional photonic crystals"*, Appl. Phys. Lett. **79**, 725-727, 2001.

[2]   A. Ovsianikov, Z. Li, J. Torgersen, J. Stampfl and R. Liska, *"Selective Functionalization of 3D Matrices Via Multiphoton Grafting and Subsequent Click Chemistry"*, Adv. Funct. Mater. **22**, 3429-3433, 2012.

[3]   J. Serbin, A. Egbert, A. Ostendorf, B. N. Chichkov, R. Houbertz, G. Domann, J. Schulz, C. Cronauer, L. Fröhlich and M. Popall, *"Femtosecond laser-induced two-photon polymerization of inorganic organic hybrid materials for applications in photonics"*, Opt. Lett. **28**, 301-303, 2003.

[4]   M. Malinauskas, P. Danilevicius, D. Baltriukiene, M. Rutkauskas, A. Žukauskas, Z. Kairyte, G. Bickauskaite, V. Purlys, D. Paipulas, V. Bukelskiene and R. Gadonas, *"3D Artificial polymeric scaffolds for stem cell growth fabricated by femtosecond laser"*, Lith. J. Phys. **50**, 75-82, 2010.

[5]   M. Maldovan and E. Thomas, *"Periodic materials and interference lithography for photonics, phononics and mechanics"*, Wiley-VCH, Weinheim, 2009.

[6]   Z. Wang, G. Zhao, W. Zhang, Z. Feng, L. Lin and Z. Zheng, *"Low-cost micro-lens arrays fabricated by photosensitive sol–gel and multi-beam laser interference"*, Photonics Nanostruct. Fundam. Appl. **10**, 667-673, 2012.

[7]   C. M. Cesa, N. Kirchgebner, D. Mayer, U. S. Schwarz, B. Hoffmann and R. Merkel, *"Micropatterned silicone elastomer substrates for high resolution analysis of cellular force patterns"*, Rev. Sci. Instrum. **78**, 034301-034310, 2007.

[8]   M. Deubel, G. Von Freymann, M. Wegener, S. Pereira, K. Busch and C. Soukoulis, *"Direct laser writing of three-dimensional photonic-crystal templates for telecommunications"*, Nat. Mater. **3**, 444-447, 2004.

[9]   D. N. Silva, M. Gerhardt De Oliveira, E. Meurer, M. I. Meurer, J. V. Lopes Da Silva and A. Santa-Bárbara, *"Dimensional error in selective laser sintering and 3D-printing of models for craniomaxillary anatomy reconstruction"*, J. Cranio-Maxillofacial Surg. **36**, 443-449, 2008.

[10]   D. Sin, X. Miao, G. Liu, F. Wei, G. Chadwick, C. Yan and T. Friis, *"Polyurethane (PU) scaffolds prepared by solvent casting/particulate leaching (SCPL) combined with centrifugation"*, Mat. Sci. Eng. C **30**, 78-85, 2010.

[11]   X. Liu and P. X. Ma, *"Phase separation, pore structure, and properties of nanofibrous gelatin scaffolds"*, Biomaterials **30**, 4094-4103, 2009.

[12]   A. Salerno, M. Oliviero, E. Di Maio, S. Iannace and P. Netti, *"Design of porous polymeric scaffolds by gas foaming of heterogeneous blends"*, J. Mater. Sci. - Mater. Med. **20**, 2043-2051, 2009.

[13]   M. Campbell, D. N. Sharp, M. T. Harrison, R. G. Denning and A. J. Turberfield, *"Fabrication of photonic crystals for the visible spectrum by holographic lithography"*, Nature **404**, 53-56, 2000.

[14]   Y. Yang, Q. Li and G. P. Wang, *"Design and fabrication of diverse metamaterial structures by holographic lithography"*, Opt. Express **16**, 11275-11280, 2008.

[15]   B.-S. Kim and D. J. Mooney, *"Development of biocompatible synthetic extracellular matrices for tissue engineering"*, Trends Biotechnol. **16**, 224-230, 1998.

[16]   M. P. Lutolf and J. A. Hubbell, *"Synthetic biomaterials as instructive extracellular microenvironments for morphogenesis in tissue engineering"*, Nat. Biotech. **23**, 47-55, 2005.

[17] E. Alsberg, H. A. Von Recum and M. J. Mahoney, *"Environmental cues to guide stem cell fate decision for tissue engineering applications"*, Expert Opinion on Biological Therapy **6**, 847-866, 2006.

[18] A. Ovsianikov, J. Viertl, B. Chichkov, M. Oubaha, B. Maccraith, I. Sakellari, A. Giakoumaki, D. Gray, M. Vamvakaki, M. Farsari and C. Fotakis, *"Ultra-Low Shrinkage Hybrid Photosensitive Material for Two-Photon Polymerization Microfabrication"*, ACS Nano **2**, 2257-2262, 2008.

[19] T. Kondo, S. Juodkazis and H. Misawa, *"Reduction of capillary force for high-aspect ratio nanofabrication"*, Appl. Phys. A **81**, 1583-1586, 2005.

[20] S. Juodkazis, V. Mizeikis and H. Misawa, *"Three-dimensional microfabrication of materials by femtosecond lasers for photonics applications"*, J. Appl. Phys. **106**, 051101-051114, 2009.

[21] I. Wang, M. Bouriau, P. L. Baldeck, C. Martineau and C. Andraud, *"Three-dimensional microfabrication by two-photon-initiated polymerization with a low-cost microlaser"*, Opt. Lett. **27**, 1348-1350, 2002.

[22] J. Serbin, *"Fabrication of photonic structures by two-photon polymerization"*, Dissertation, Cuvillier Verlag, Gottingen, 2004.

[23] H. Ottevaere, R. Cox, H. P. Herzig, T. Miyashita, K. Naessens, M. Taghizadeh, R. Völkel, H. J. Woo and H. Thienpont, *"Comparing glass and plastic refractive microlenses fabricated with different technologies"*, J. Opt. A: Pure Appl. Opt. **8**, S407-S429, 2006.

[24] V. Keskar, N. W. Marion, J. J. Mao and R. A. Gemeinhart, *"In Vitro Evaluation of Macroporous Hydrogels to Facilitate Stem Cell Infiltration, Growth, and Mineralization"*, Tissue Eng. Part. A **15**, 1695-1707, 2009.

[25] J. M. Eisenhart and A. B. Ellis, *"Perturbation of the excited-state properties of trans,trans-1,5-bis[4-(dimethylamino)phenyl]-1,4-pentadien-3-one through adduct formation and silica gel adsorption"*, J. Org. Chem. **50**, 4108-4113, 1985.

[26] M. S. Hahn, J. S. Miller and J. L. West, *"Three-Dimensional Biochemical and Biomechanical Patterning of Hydrogels for Guiding Cell Behavior"*, Adv. Mater. **18**, 2679-2684, 2006.

CURRICULUM VITAE

Name, Surname: **Evaldas Stankevičius**

Date of birth and place: **1982 04 22**, Klaipėda, Lithuania

Education: **2000** Klaipėdos "Varpo" secondary school

                                  2004 Physics Bachelor Degree of Vilnius University

                                  2006 Physics Master Degree of Vilnius University

                                  2009-2013 PhD studies at the Center for Physical Sciences and Technology, Institute of Physics, Lithuania

Santrauka

Disertacijos tikslas buvo sukurti metodą periodinių darinių formavimui interferencinės litografijos būdu, polimerizuojant fotojautrias medžiagas, eksperimentiškai ištirti šio metodo galimybes ir ribojimus bei suformuoti mikrodarinius, tinkamus praktiniams taikymams.

Eksperimentų metu buvo pademonstruota, kad interferencinės litografijos metodu formuojamų mikrodarinių forma priklauso nuo: lazerinės apšvitos dozės, bangos ilgio, fazės, kampo tarp interferuojančių pluoštų ir pluoštų skaičiaus, o jų tvirtumas labiausiai priklauso nuo lazerinės apšvitos dozės.

Šiame darbe taip pat parodyta, kad naudojant interferencinės litografijos metodą viena lazerine ekspozicija galima formuoti mikrovamzdelių ir mikrolęšių masyvus bei karkasus iš biosuderinamos ir biosuskaidomos PEG-DA-258 medžiagos.

Be polimerinių darinių formavimo, šiame darbe pademonstruota ir jų fotomodifikavimo galimybė, naudojant fotoįskiepijimo (angl. photo-grafting) technologiją, o taip pat realizuojant variu katalizuojamos azido alkino ciklizacijos (CuAAC) cheminę reakciją parodyta fotoįskiepijimo technologijos ir „klik“ chemijos apjungimo galimybė. Toks paprastas ir universalus būdas atveria naujas galimybes biojutiklių kūrime ir audinių inžinerijoje, nes molekulių imobilizavimas polimero matricoje vyksta trimatėje erdvėje ir tiksliai norimoje vietoje, o trimatė erdvinė gradientinė kontrolė yra labai svarbi daugybėje biotechnologijos taikymų.

Dalis darbe atliktų eksperimentų turi praktinę vertę, kadangi interferencinės litografijos metodas leidžia greitai ir efektyviai suformuoti mikrodarinius (mikrolęšių, mikrovamzdelių, karkasų), tinkamus įvairioms sritims (mikrooptikai, mikrotėkiams ar audinių inžinerijai) bei juos modifikuoti (fotoįskiepijimas).